

Advances in Technology and Design of Ultra Wideband millimeter wave planar and non-planar duplexers for applications up to 100GHz

Irfan Ashiq, Utkarsh Unnikrishna and A.P.S Khanna, Fellow, IEEE

National Instruments Inc.

4600 Patrick Henry Drive, Santa Clara, CA 95054 USA

Abstract — This paper will discuss implementation of several planar and non-planar ultrabroad band contiguous and non-contiguous diplexer designs at millimeter wave frequencies up to 100 GHz. The duplexers discussed are realized either using Suspended Stripline (SSL) or combination of SSL and E-plane waveguides. These duplexers meet stringent performance requirements for applications such as broadband signal acquisition systems (real-time oscilloscopes) and at component level application such as millimeter wave mixers where frequency splitting is required for IF and LO. The system level performance parameters include symmetrical steep band selectivity with low in band insertion loss. Also maintaining better than 12dB return loss and phase linearity at the crossover frequencies which becomes difficult at millimeter waves above 30GHz. The paper will also highlight use of exotic organic dielectric materials for design of contiguous duplexers up to 100GHz on planar SSL technology.

Index Terms — Liquid Crystal Polymer, Suspended Stripline, contiguous diplexer, soft-board, recessed cavity, lowpass filter, highpass filter, millimeter wave diplexer.

I. INTRODUCTION

In the past significant work has been done on non-contiguous and contiguous multiplexers upto 110GHz [1]. The multiplexer filter at mm-Wave frequencies were dominantly implemented using suspended probes to a waveguide transition. In other words the design was not purely planar using homogeneous dielectric material. In case of contiguous duplexers, the synthesis of singly terminated filters for duplexers have significantly evolved over period of time in planar domain. Specifically, the cross-coupled or broad-side coupling on suspended stripline has made it very practical to implement complementary filters with high coupling coefficients and quality factor and minimizing losses at the cross-over frequency regions [2].

These days, emerging applications of mm wave technologies require new and higher performance components and test equipment. These applications include Broadband wireless, high-speed wired, Automobile Radars, Imaging and wireless sensors. 5G wireless systems are expected to take full advantage of wide bandwidths available in mm wave region. Test equipment needs to keep ahead of the devices under test. All these applications require components with small-size and excellent electrical performance [1]. Stringent requirements need to be imposed on the underlying material technologies.

This work will discuss design of mmWave planar and non-planar contiguous and non-contiguous singly terminated duplexers and performance parameter comparison.

II. APPLICATIONS OF MM-WAVE DIPLEXERS

Figure 1 shows a typical application of planar DC-67-100GHz[3] and planar DC-35-67GHz[4] are implemented as a key component in the mm-Wave frond-end for a real-time 100 GHz oscilloscope design.

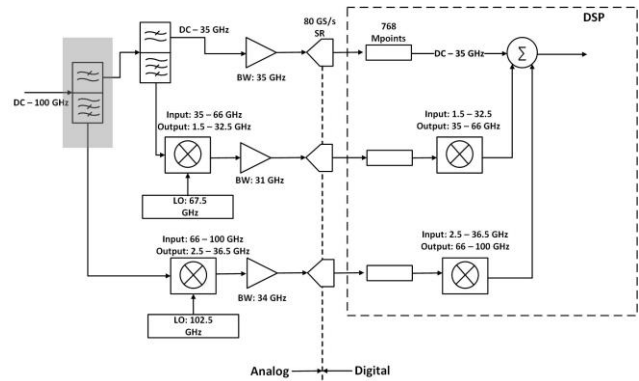


Fig. 1. Digital Bandwidth Interleaving (DBI) System Block Diagram

The two duplexers in microwave front-end as shown in fig. 1 separate the incoming broadband signal DC – 100 GHz into three frequency bands (DC to 35 GHz, 35 to 67 GHz, and 66 to 100 GHz). The higher frequency bands are block down-converted to a frequency range suitable for acquisition by digitizing channels in DSP block as shown in the figure. In this design, three 36 GHz, 80 GS/s scope channels are utilized.

In Digital Bandwidth Interleaving, or DBI in which multiple channel resources are combined to an oscilloscope channel that is virtually a combination of the bandwidths of the combined channels. DBI increases both bandwidth and sample rate. In this DBI system, the digitized bands are stitched back to re-create a 100GHz, 240 GS/s waveform acquisition [5]. DC-35-67GHz and DC-67-100GHz diplexer are employed in form of a triplexer by cascading them in series as shown in Fig1. They are the key components which enable DBI application

As for the application of non-contiguous diplexer, a typical application is in a mm-Wave mixer where frequency separation of LO and IF signals is done by means of a stand-alone three-port non-contiguous diplexer. The mixer for this design is uniplanar and typically covers RF bandwidth of 33 to 67GHz with IF bandwidth of 0.5 to 34GHz. The diplexer is implemented on Suspended Stripline (SSL) technology with 5 mil dielectric substrate ($\epsilon_r = 2.1$)[8].

As shown in figure 2, the common port of the diplexer connects to the output CPW of the mixer and passes the LO and IF signals. The low-pass filter of the diplexer outputs the IF signal from the mixer and the bandpass filter allows the LO signal into the mixer from 55 to 68GHz[8].



Fig. 2: Mixer-Diplexer assembly

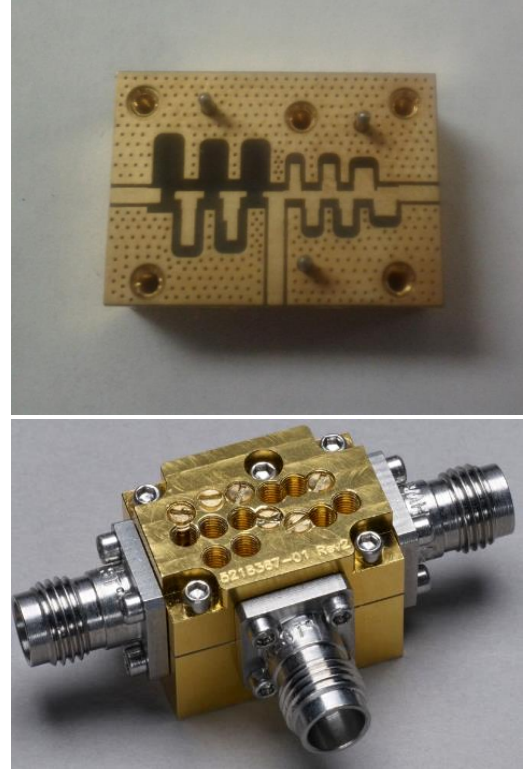


Fig 3. Diplexer suspended substrate and assembly

Figure 4 below shows measured results of the planar DC-35-67GHz diplexer, where S11 is the input return loss, S21 is the insertion loss of the lowpass and S31 is the insertion loss of the highpass [3].

III. DESIGN AND SPECIFICATION COMPARISON OF PLANAR AND NON-PLANAR (HYBRID) DC-35-66 GHz DIPLEXER

A. Design and measured results for planar approach

In case of the planar diplexer as shown in figure 3, the lowpass is implemented using Tchebyshev 13th order stepped impedance design is implemented using series $\lambda/8$ high impedance and shunt $\lambda/2$ low impedance resonators. The cutoff frequency of the filter is set to 35GHz with pass-band ripple of 0.1dB.

The highpass is based LC lumped element prototype circuit of the Tchebyshev 11th order with corner frequency at 35 GHz. The series capacitances of the high-pass are implemented using broadside coupled strip elements on either side of the substrate. The shunt inductances are implemented using short circuited step impedance line resonators with nominal electrical length of $\lambda/2$ [3], [5]. Physical lengths of the resonators and overlap sections of highpass filter are finely optimized in CST for the required performance.

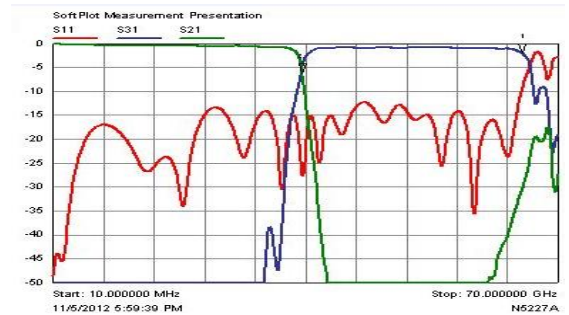


Fig 4. Planar DC-35-67GHz diplexer measured result

B. Design and measured results for non-planar approach

The lowpass filter is very similar to the lowpass in planar diplexer using Tchebyschev lowpass 13th order stepped impedance lowpass design is synthesized by implementing series $\lambda/8$ high impedance (120 ohms) and shunt $\lambda/2$ low impedance (70 ohm) resonators. The cutoff frequency (f_0) of the filter is set to 36 GHz with pass-band ripple of 0.1 dB.

The highpass filter from the common input junction of the diplexer is implemented by a single capacitive broadside coupled section that is connected to a resonator stub that forms a H-plane probe transitioning into a non-standard waveguide. This probe on a dielectric substrate is suspended in a rectangular waveguide. The input broadband signal is propagated in TEM mode in SSL structure, which then converts to dominant TE_{10} when launched through a probe into the waveguide as shown in figure 5.

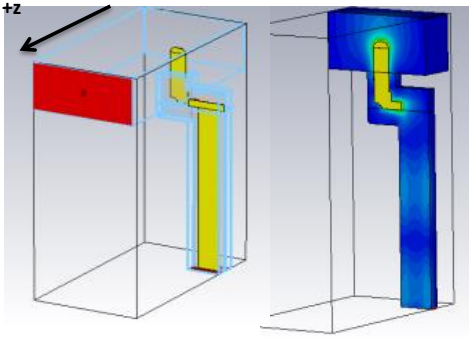


Fig. 5. Highpass filter in non-standard waveguide

The a and b dimensions of the waveguide are chosen such that TE_{10} cutoff frequency of the guide is 36 GHz, calculated from equation (4) and its wave impedance computed from equation (5).

$$f_{cTE_{10}} = c/2a \quad (1)$$

$$Z_{TE_{10}} = \frac{\sqrt{\frac{\mu}{\epsilon}}}{\sqrt{1-f_c^2/f^2}} \rightarrow \sqrt{\frac{\mu}{\epsilon}} \quad (2)$$

The dimensions for the waveguide were chosen to be 82 mils x 164 mils. Since the dimensions are non-standard, a transition from non-standard waveguide to SSL and finally to coax was designed to enable a complete broadband response from DC-66 GHz. The complete assembly of the hybrid diplexer and measured results are shown in figures 6 and 7 [5].



Fig. 6: Complete assembly of DC-35-67GHz hybrid diplexer

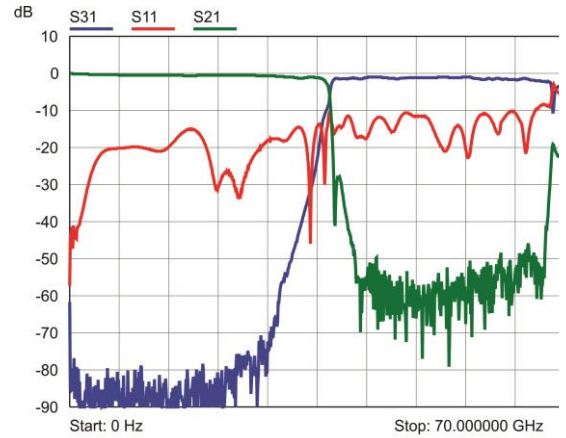


Fig. 7: Measured results

C. Performance Comparison

Both diplexer designs planar and non-planar exhibit excellent flatness. Return loss better than 10 dB was measured across the band. In case of the hybrid or the non-planar diplexer, it displays 3% higher fractional bandwidth which 63% in highpass compared in planar diplexer that is 60%. The hybrid diplexer also exhibits high band selectivity of 25dB within ± 2 GHz bandwidth of the crossover frequency which is 5dB better compared to planar approach.

IV. DESIGN AND SPECIFICATION COMPARISON OF PLANAR AND NON-PLANAR (HYBRID) DC-66-100 GHz DIPLEXER

Choice of dielectric material was a critical step in implementing contiguous diplexer performing upto 100GHz. The planar substrate used for the diplexer is Roger’s Ultralam 3850 material with dielectric constant of 2.9, and effective dielectric constant is closer to 1 due to SSL structure. The substrate thickness is only 0.002 in. With such low substrate thickness, implementing high Q and low capacitance values on broadside coupled sections becomes more practical due to SSL, especially at millimeter-wave frequencies.

D. Design and measured results for planar approach

The planar lowpass filter was implemented with 13th order stepped impedance design is implemented using series $\lambda/8$ high impedance and shunt $\lambda/2$ low impedance resonators. The cutoff frequency of the filter is set to 67 GHz with pass-band ripple of 0.1 dB. Where as the highpass filter was realized by synthesizing 11th-order at 35GHz corner frequency. The series capacitances of the highpass are implemented using broadside coupled strip elements on either side of the substrate. The shunt inductances are implemented using short-circuited step impedance line resonators with a nominal electrical length of $\lambda/2$ as shown in figure 8.

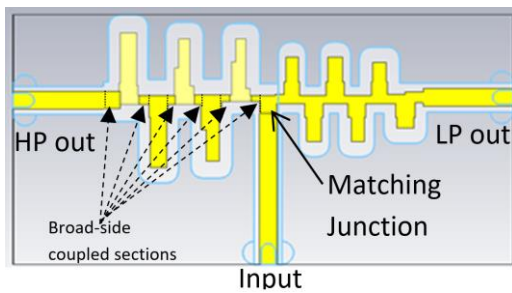


Fig. 8: Lowpass and Highpass sections of planar diplexer

Figure 9 and 10 shows the complete assembly of the diplexer with the measured results of log magnitude input port match (S11), lowpass (S21) and highpass (S31). The measured response in fig. 10 is shown with final post tuning implemented using sapphire rods. As this tuning technique provides fine capacitive and inductive compensation at the edges of the resonators and broadside coupled sections of the lowpass and highpass circuits of the diplexer. The T-junction or the matching junction can also be tuned with the rods for optimal performance [4].

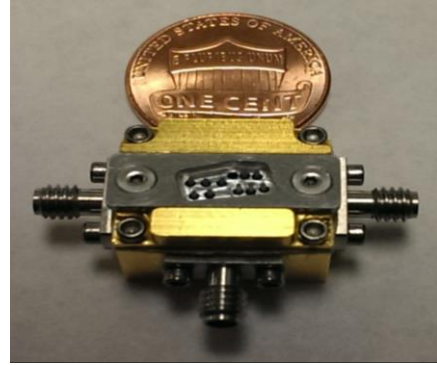


Fig. 9: Complete assembly of DC-67-100GHz planar diplexer

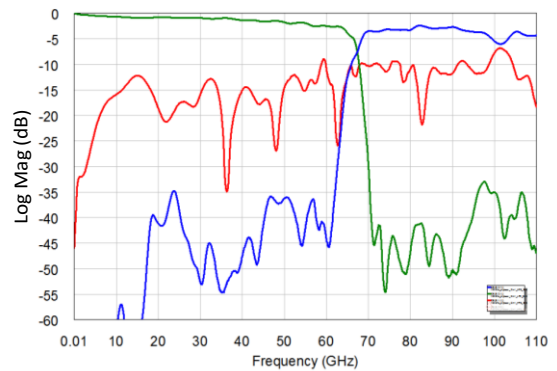


Fig. 10: Measured results of DC-67-100GHz planar diplexer

E. Design and measured results for non-planar approach

The lowpass filter in the non-planar DC-67-100GHz was implemented using LCP 0.002” thick material and synthesizing 13th order stepped impedance series $\lambda/8$ high impedance and shunt $\lambda/2$ low impedance resonators. From the common input junction of the diplexer there is a single capacitive broadside coupled section that is connected to a resonator stub or a probe. This probe on a dielectric substrate is suspended in a rectangular waveguide as shown in Fig 11, that forms a highpass filter of the diplexer. The input broadband signal is propagated in TEM mode in SSL structure, which then converts to dominant TE_{10} when launched through a probe into the waveguide. The transition must achieve both mode conversion and impedance matching between the SSL and waveguide. A probe placed in the center of the E-plane of the waveguide efficiently captures the electromagnetic energy [9].

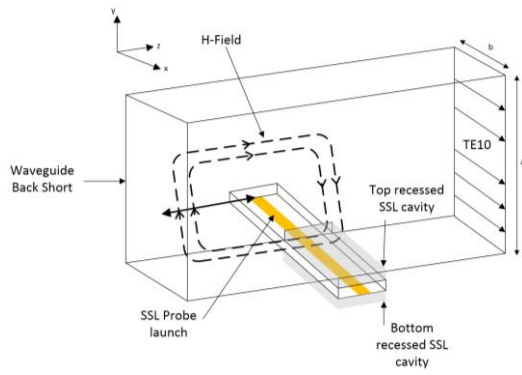


Fig. 11: Highpass section of DC-67-100GHz hybrid diplexer

In order to ensure maximum energy flow in the TE_{10} mode, the distance of the probe to the back short is optimized. The electrical distance between the probe and the short needs to be one quarter of guide wavelength $\lambda_g/4$ (at center of high-pass frequency range) in order to maximize RF energy in the z+ direction.

The complete diplexer combined along with the tapered transition at the output of the HPF into WR-10 was simulated and shown in Figure 12 and mechanical assembly. Measured log magnitude of the S-parameters of the diplexer are shown in figure 13.

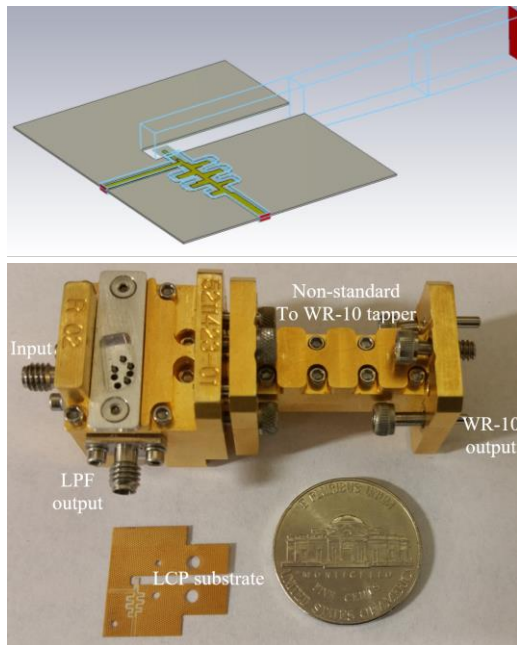


Fig. 12: Complete assembly of DC-67-100GHz diplexer

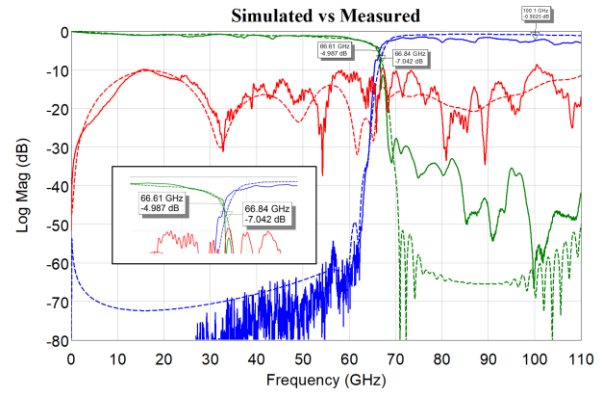


Fig. 13: Simulation vs. Measured results

F. Comparison

Below table 1 shows comparison of parameters of the performance parameters for planar versus non-planar (hybrid) diplexer.

Performance parameters	Planar	Non-Planar
Insertion loss at cross-over (dB)	7.5 (67GHz)	5 (67GHz)
Input port match (dB)	>9 (DC-100GHz)	>10 (DC-100GHz)
Band selectivity +/- 2GHz from cross-over (dB)	>20 (67GHz)	>30 (67GHz)
Highpass max frequency (GHz)	100	110

Table 1: Performance parameter comparison of planar and non-planar diplexer

Non-planar takes an edge in terms of low insertion loss, higher frequency performance in a highpass response, better input match and steep band selectivity

V. DESIGN OF NON-CONTIGUOUS PLANAR DIPLEXER COVERING BANDS DC-34GHz AND 55GHz - 68GHz

A broadside-coupled diplexer in Suspended StripLine technology (SSL) implemented on RO5880 dielectric material. The lowpass and bandpass channels are required cover wide bandwidth of DC-34GHz and 55GHz to 68GHz.

G. Lowpass Filter:

The Tchebyscheff lowpass section of the diplexer is synthesized using iFilter feature in AWR. The 13th order stepped impedance lowpass design is synthesized by

implementing series $\frac{\lambda}{8}$ high impedance (120ohms) and shunt $\frac{\lambda}{2}$ low impedance (70 ohm) resonators. The cutoff frequency (f_0) of the filter is set to 32GHz with passband ripple of 0.1dB.

H. Bandpass Filter Model and design steps:

The fast synthesis of the band pass is modeled from $\frac{\lambda}{2}$ resonators with overlapped gaps on either ends that form an equivalent π networks as shown in Fig 14.

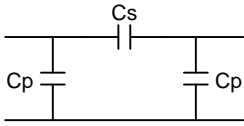


Figure 14: Equivalent π network of the overlap region between two resonators
Where C_s and C_p are the series and parallel capacitances of the overlap region $l_{overlap}$. The resonators are realized with line impedances higher than 80 ohms.

For the bandpass filter resonator line widths are fixed to control the line impedance of each section. Before EM simulating all coupled sections, select one section at a time and extract Y-matrix after de-embedding the reference planes of the waveguide ports to the middle of the gap as shown in Fig. 15.

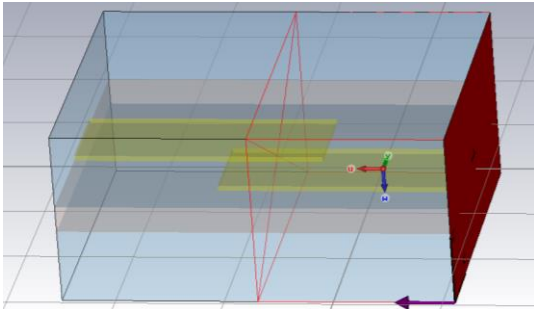


Figure 15: Overlap section with waveguide ports de-embedded to the middle of the coupled region.

The C_s and C_p values are computed from equations (9) and (10). Since the coupled section is symmetrical hence follows the rule of reciprocity. Which means $Y_{11} = Y_{22}$ and $Y_{21} = Y_{12}$. The extracted C_s for all coupled sections can then be compared with the computed closed-form C_s values in step 4.

$$C_s = j \frac{y_{21}|_{f=f_0}}{2\pi f_0} \quad (9)$$

$$C_p = j \frac{(y_{11} + y_{21})|_{f=f_0}}{j2\pi f_0} \quad (10)$$

The physical lengths of the resonators and overlap sections of bandpass filter are finely optimized in CST for the required performance. Figure 16 shows the complete assembly of the diplexer and the measured results.

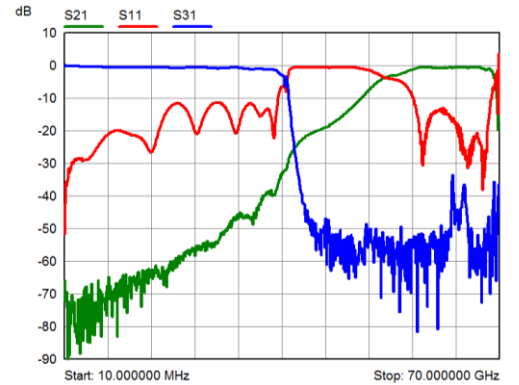


Fig. 16: Measured response of non-contiguous diplexer

VI. PHASE LINEARITY OF MM-WAVE CONTIGUOUS DIPLEXER

One of the sensitive parameters in optimal performance of contiguous diplexer is phase linearity around the cross over region of the diplexer. In the digital data acquisition application or for merging frequency bands, the low pass and high pass S-parameters in vector form are required to add up in magnitude to compensate the loss at cross over of the contiguous diplexer. The sum of the magnitudes of vector can add up constructively, if and only if both low pass and high pass vectors are within 90 degrees of each other. this relationship as shown in equation 11.

$$|\overline{S_{LP+HP}}| > |\overline{S_{LP}}| \text{ and } |\overline{S_{HP}}| \quad (11)$$

VIII. REFERENCES

- [1] Shih, Bui, "Millimeter-Wave Diplexer With Printed Circuit Elements", IEEE 1985
- [2] R. Levy, "Synthesis of general asymmetric singly and doubly terminated cross-coupled filters" IEEE Transaction and Microwave Theory and Techniques, Vol. 42, No. 12, December 1994
- [3] I. Ashiq and Khanna, "Ultra-Broadband Contiguous Planar DC-35-65 GHz Diplexer using Softboard Suspended Stripline Technology" IMS 2013, Seattle, WA.
- [4] I. Ashiq and Khanna, "A Novel Planar Contiguous Diplexer DC-67-100GHz Using Organic Liquid Crystal Polymer (LCP)" IMS 2015, Phoenix, FL.
- [5] I. Ashiq and A. Khanna, "A Novel Ultra-Broadband DC-36-66GHz Hybrid Diplexer Using Waveguide and SSL Technology" Pg. 1111, 44th European Microwave Conference, Rome, Italy, Oct. 2014.
- [6] X. Chen, S. Chandrasekhar, P. Winzer, P. Pupalais, I. Ashiq, A. Khanna, A. Steffan, and A. Umbach, "180-GBaud Nyquist Shaped Optical QPSK Generation Based on a 240-GSa/s 100-GHz Analog Bandwidth DAC" Asia Communications and Photonics Conference 2016, in Wuhan
- [7] Irfan Ashiq and Amarpal Khanna, "Ultra Broadband Non-Planar DC-67-100GHz Contiguous Diplexer Implemented On Organic Liquid Crystal Polymer (LCP)", European Microwave 2016 London
- [8] Alexander Feldman, Utkarsh Unnikrishna, Irfan Ashiq and Amarpal Khanna, "An Ultra-Broadband Planar Millimeter-Wave Mixer with IF Bandwidth covering 0.5 to 34 GHz", Proceedings of the 44th European Microwave Conference October 2014 in Rome, Italy
- [9] Amarpal Khanna and Irfan Ashiq, "Ultra Broadband Diplexer Using Waveguide and Planar Transmission Lines", Patent US9252470B2, 02/02/2016

In theory, the phase difference between lowpass and highpass vectors is required to be constant around the cross-over region. However, in practice the phase difference can vary, as long as this phase difference remains within 0 to 90 degrees. Figure 17 shows the measured phase in 2GHz bandwidth around the crossover. The vertical lines on the plot indicate cross-over region at frequencies 65.5 GHz, 66.6 GHz, and 67.6 GHz. This measurement was taken on hybrid DC-67-100 GHz diplexer. At mmWave frequencies it gets challenging to achieve the conditions stated in equation 11.

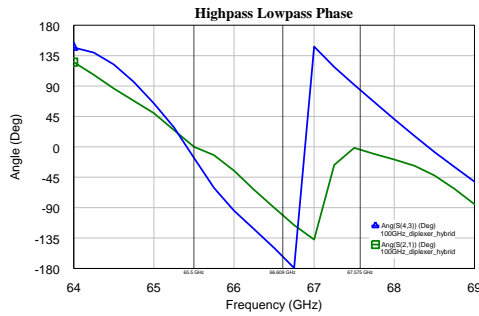


Fig. 17: Lowpass and Highpass phase response versus frequency

Figure 18 displays phase difference in degrees ($\vec{S}_{HP} - \vec{S}_{LP}$) in between the lowpass (in green) and high pass (in blue) vectors as shown in figure 17.

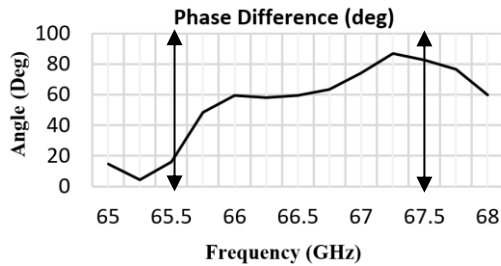


Fig. 18. Phase difference in degrees ($\vec{S}_{HP} - \vec{S}_{LP}$)

VII. CONCLUSION

A high-performance mmWave planar and non-planar contiguous and non-contiguous diplexer designs and their key applications had been detailed in this paper. In terms of design comparison, both planar and non-planar approaches exhibited their own advantages and disadvantages, but non-planar diplexer design take a edge in terms of critical parameters such as low insertion loss, high-band selectivity and higher fractional bandwidth and frequency performance. This work also highlighted detailed design of a mmWave planar non-contiguous diplexer for specific applications.